Spreading Resistance as a Function of Frequency

LAWRENCE E. DICKENS, MEMBER, IEEE

Abstract—**The equivalent circuit applicable to most semiconductor diodes contains a term R_s called the spreading resistance which is a very critical parameter of any diode. In a mixer diode, R_s limits the conversion efficiency and increases the noise temperature. In parametric amplifiers, R_s affects the overall impedance levels and determines the minimum noise figure of which the amplifier is capable. In harmonic generators it drastically affects the conversion efficiency, as it dissipates power not only at the input and output harmonic frequencies but also at every idler frequency for which current may flow through the diode.**

This paper details more specifically the problems encountered when high frequency operation must be evaluated. The cylindrical capacitor is examined with emphasis on the configuration which applies to the variable-capacitor diode, which is used primarily for harmonic power generation.

The point-contact diode configuration is examined and the field equations are derived in terms of the oblate spheroidal coordinates. It is shown that this is the natural coordinate system for such an analysis and that the spreading resistance is quite easily derived in this system.

I. Introduction

THE EQUIVALENT circuit applicable to most semiconductor diodes contains a term R_s called the spreading resistance which is a very critical parameter of any diode. In a mixer diode, R_s limits the conversion efficiency and increases the noise temperature. In parametric amplifiers, R_s affects the over all impedance levels and determines the minimum noise figure of which the amplifier is capable. In harmonic generators it drastically affects the conversion efficiency, as it dissipates power not only at the input and output harmonic frequencies but also at every idler frequency for which current may flow through the diode.

The calculation of R_s becomes a problem with geometrical dependence, and, as skin effect will play a dominant role in the control of the flow of high-frequency electric current, the calculations must accurately include this effect. In all the cases to be considered in the following sections, cylindrical symmetry will be maintained in the device configuration as an aid to computation; however, this imposes no limitations as it is a thoroughly practical assumption.

This paper presents the theory of skin effect as it applies to parametric (capacitor) diodes and point-contact diodes. Most references give no more than a passing glance at the subject of skin effect; thus, credit must be given to the text by King [1] which is most notable for its completeness.

Manuscript received August 13, 1965; revised December 20, 1965. This work was supported by the National Aeronautics and Space Administration through Contract NAS 5-3546, and the Air Force Avionics Laboratory through Contract AF 33(657)-11029.

The author is with the Advanced Technology Corporation, Timonium, Md. He was formerly with The Johns Hopkins University Carlyle Barton Laboratory, Baltimore, Md.

II. Skin Effect and RF Impedance

The constriction of current flow through a small disk electrode and the calculation of the resulting distribution is sufficiently complicated at zero frequency that the use of high speed computers is the only feasible way of obtaining any amount of data. This has already been demonstrated in another paper [2]. With the consideration of high-frequency operation, one must consider the influence of skin effect[1] and the degree to which it forces the further constriction of the current to the outermost surfaces of the region of current flow.

A. Field Equations

As the current distributions maintain general rotational symmetry and in particular all configurations maintain cylindrical symmetry, all the formulas for the field will be derived subject to this restriction.

1) *General Rotational Symmetry:* Given the system of coordinates (ξ, η, θ) with rotational symmetry, the metrical coefficients are defined by the equation

$$ds^2 = h_1^2 d\xi^2 + h_2^2 d\eta^2 + r^2 d\theta^2 \tag{1}$$

where r is the perpendicular distance from the axis of rotation. If the field has the same symmetry as the coordinate systems, its components are independent of θ, and, following Stratton [4] one finds that

$$\text{curl } E = -j\omega\mu H \tag{2}$$

and

$$\text{curl } H = (\sigma + j\omega\epsilon)E = \frac{\gamma^2 E}{j\omega\mu} \tag{3}$$

break up into the following set (for $H = H_\theta \theta$)

$$\frac{1}{rh_2}\frac{\partial}{\partial\eta}(rH_\theta) = \frac{+\gamma^2}{j\omega\mu}E_\xi, \tag{4}$$

$$\frac{1}{rh_1}\frac{\partial}{\partial\xi}(rH_\theta) = \frac{-\gamma^2}{j\omega\mu}E_\eta, \tag{5}$$

$$\frac{1}{h_1 h_2}\left[\frac{\partial}{\partial\xi}(h_2 E_\eta) - \frac{\partial}{\partial\eta}(h_1 E_\xi)\right] = -j\omega\mu H_\theta, \tag{6}$$

and that these relations are satisfied by the scalar function Q which is defined as

$$Q = rH_\theta. \tag{7}$$

[1] Skin effect has been concisely defined by Holm [3]: "The effect consists of an induction by the current's own magnetic field pressing the lines of flow toward the exterior of the conductor, thus diminishing the effective conducting cross section and increasing the resistance."

Then, in terms of Q, the electric intensities are given as

$$E_\xi = \frac{j\omega\mu}{rh_2\gamma^2}\frac{\partial Q}{\partial \eta} \tag{8}$$

and

$$E_\eta = \frac{-j\omega\mu}{rh_1\gamma^2}\frac{\partial Q}{\partial \xi}. \tag{9}$$

The resulting second order, linear, partial differential equation that is obtained is

$$\frac{\partial}{\partial \xi}\left(\frac{h_2}{rh_1}\frac{\partial Q}{\partial \xi}\right) + \frac{\partial}{\partial \eta}\left(\frac{h_1}{rh_2}\frac{\partial Q}{\partial \eta}\right) - \gamma^2\frac{h_1h_2}{r}Q = 0. \tag{10}$$

2) *Cylindrical Coordinates:* Now if cylindrical symmetry is encountered so as to make desirable the use of the cylindrical coordinate system, we take $\xi = r$, the radial component; $\eta = z$, the axial component; and $\theta = \theta$, the angular component. The metrical coefficients are then $h_1 = h_2 = 1$, and $r = r$. The differential equation takes the form shown in (11).

$$\frac{\partial^2 Q}{\partial r^2} - \frac{1}{r}\frac{\partial Q}{\partial r} + \frac{\partial^2 Q}{\partial z^2} - \gamma^2 Q = 0. \tag{11}$$

The solution to (11) is of the form

$$Q(z) = Ce^{\pm kz} \tag{12}$$

and

$$Q(r) = C_1 r J_1(\beta r) \tag{13}$$

where the Neumann function is not allowed, and

$$\beta = \sqrt{k^2 - \gamma^2}. \tag{14}$$

From (8) and (9) the electric intensities are found to be

$$E_r = \pm\frac{j\omega\mu}{\gamma^2} krJ_1(\beta r)e^{\pm kz}A_1 \tag{15}$$

and

$$E_z = -\frac{j\omega\mu}{\gamma^2}\beta J_0(\beta r)e^{\pm kz}A_2, \tag{16}$$

where A_1 and A_2 are scale factors yet to be determined. Similarly, the magnetic intensity, obtained from (7) and (16), is found to have the form

$$H_\theta = A_3 J_1(\beta r). \tag{17}$$

B. Cylindrical Capacitor

A most interesting problem in the consideration of diode resistance is the determination of the spreading resistance of the diode capacitor. This R_s is most critical in two diode capacitor applications. The first application is to the low noise parametric amplifier in which it represents the primary noise source. The second application is to the varactor (variable reactor) harmonic power generator. For the first application, the radius a of the contact is equal to, or less than, the skin depth in the metal wire contact and is much less than the skin depth in the semiconductor. In the second application, the radius of the contact surface is much greater than the skin depth of the metal contact and in most instances of practical importance can be considered to be much greater than the skin depth in the semiconductor also. This last statement must usually be qualified by closer consideration of the terminal frequencies involved as there may be as much as an order of magnitude difference between the signal and pump (and idler) frequencies of the parametric amplifier and also between the input and harmonic frequencies of the multiplier.

The question of the operation of the point-contact diode will be put off until a later section. There it will be treated with the assumption of equipotential contact surface.

A complete formulation of the broad area contact problem is prohibitively complex but the important characteristics of the circular, back-biased junction may be derived by assuming it to be a circular, planar capacitor. Consider a capacitor consisting of two parallel circular plates of conductivity σ_1 and σ_2. The plates are separated by a narrow region of width d called the depletion layer [6], [7] the width of which we will assume to be determined and fixed by an applied reverse-bias potential. This arrangement may be represented as shown in Fig. 1.

The plates (1 and 2) have been shown as having different widths as well as different conductivities. The region 1 may approximate the large area (volume) dot or disk which would be used in the usual alloy junction forming process. The region 2 represents the basic semiconductor wafer. The region 3 then represents the regrowth (junction) location.

The z axis is the axis of symmetry, and it is safe to assume that the width of the depletion layer d is very small compared with either radius a or b and with the wavelength. That is

$$d \ll a \leq b; \qquad d \ll \lambda; \tag{18}$$

hence, edge effects may be neglected, and the electric and magnetic intensities of region 3, E_{z3} and $H_{\theta 3}$, can be taken to be independent of z, and (16) and (17) hold, i.e.,

$$E_{z3}(r) = E_{z3}(a)\frac{J_0(\beta r)}{J_0(\beta a)}, \tag{19}$$

and

$$H_{\theta 3}(r) = H_{\theta 3}(a)\frac{J_1(\beta r)}{J_1(\beta a)}. \tag{20}$$

By application of the circuital law,

$$\oint_c H\,dl = (\sigma + j\omega\epsilon)\int_{s(\text{cap})} E\,ds, \tag{21}$$

the amplitudes $E_{z3}(a)$ and $H_{\theta 3}(a)$ may be obtained in terms of the total current I_{z1} entering or leaving the interface between regions 1 and 3. Thus,

$$H_{\theta 3}(r) = \frac{I_{z1}}{2\pi a}\frac{J_1(\beta r)}{J_1(\beta a)}, \tag{22}$$

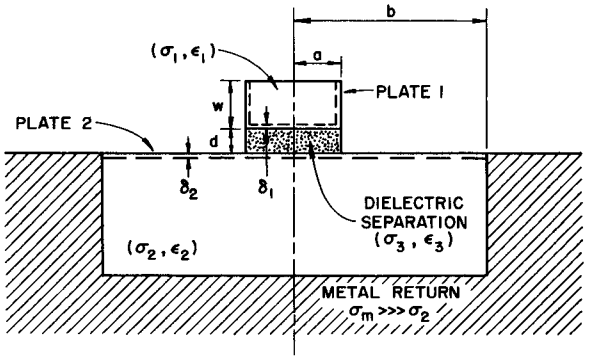

Fig. 1. Diode capacitor representation.

and

$$E_{z3}(r) = \frac{j\omega\mu}{\gamma^2}\frac{I_{z1}}{\pi a^2}\left(\frac{\beta a}{2}\right)\frac{J_0(\beta r)}{J_1(\beta a)}. \tag{23}$$

Now we have taken this to be the case, that the frequency is sufficiently high that the thickness of the plates and their radii are large compared to the skin depth (δ_1, δ_2) as shown in Fig. 1. Then it may be assumed that most of the current flowing in region 1 flows in a thin layer δ_1 radially along the inner surface of the conducting region at the interface to region 3, around the edges and then axially (in region 1) just as was determined for the long cylindrical wire. Similarly, the current flowing in region 2 flows in a thin layer δ_2 radially along the inner surface of the conducting region at the interface to region 3, and then directly radially to the return surface at $r=b$.

The radial current, $I_{r1}(r)$, at the interface can be determined by a second application of the circuital law by taking the cap surface to consist of a circular plate of radius r parallel to the interface of regions 1 and 3, but deep within region 1, and of a cylinder of radius r through which the radial current flows. As the plate is deep within the conductor (region 1) the integral over this surface is essentially zero. And then

$$H_{\theta 3}(r) = \frac{I_{r1}(r)}{2\pi r}; \tag{24}$$

but using (22) we obtain

$$I_{r1}(r) = I_{z1}\left(\frac{r}{a}\right)\frac{J_1(\beta r)}{J_1(\beta a)}, \tag{25}$$

which can be considered the total quasi-surface current flowing radially at the radius r. The surface current density $I_r^s(r)$ is then defined as the total radial current traversing a unit circumference, i.e.,

$$I_r^s(r) = \frac{I_{z1}}{2\pi a}\frac{J_1(\beta r)}{J_1(\beta a)}. \tag{26}$$

It has been shown,[2] that when the above imposed conditions are satisfied, that a surface impedance may be derived for regions 1 and 2 which is

[2] See King [1], ch. V, sec. 13.

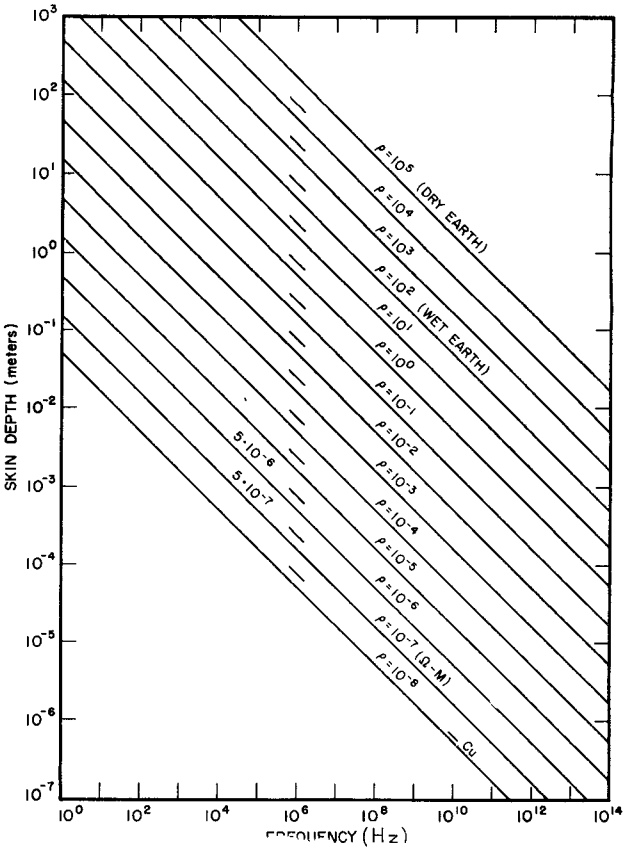

Fig. 2. Skin depth d_s versus frequency.

$$Z_s = \frac{1+j}{\sigma d_s} = R^s + jX^s, \tag{27}$$

where d_s is the traditional "skin depth" given by

$$d_s = \sqrt{\frac{2}{\omega\mu\sigma}}. \tag{28}$$

A broad range of values of d_s versus frequency and σ is presented in Fig. 2.

The average power dissipated per unit area of surface is Δp,

$$\Delta p = \tfrac{1}{2}R^s(I_r^s)^2. \tag{29}$$

Equation (29) is an expression for the I^2R loss which can be evaluated and to which an equivalent R_s can be assigned. The evaluation is performed in several parts. First the contribution to R_s (call it R_{13}^s) from only the interface between regions 1 and 3 is evaluated. Then that contribution R_{32}^s at the interface between regions 2 and 3 is similarly obtained. The contribution due to the axial flow in region 1, R_{ax}^s, is just the skin effect resistance of a simple cylindrical conductor. The contribution due to the surface flow in region 2, but outside the radial limitation of $r=a$, is the final term, call it R_{sk}^s.

Then by (26), (27), and (29) there is obtained

$$P = \frac{1}{2}\int_0^a R^s(I_r^s)^2 2\pi r\, dr = \frac{1}{2}R_{13}^s I_{z1}^2. \tag{30}$$

The factor $(\frac{1}{2})$ is used before the second two terms because of the convention wherein I refers to peak quantities. Now $R_{13}{}^s$ is obtained from (30) and is found to be

$$R_{13}{}^s = \frac{1}{4\pi d_s\sigma_1}\left[1 + \frac{J_0{}^2(\beta a)}{J_1{}^2(\beta a)}\left(1 - \frac{2}{\beta a}\frac{J_1(\beta a)}{J_0(\beta a)}\right)\right]. \quad (31)$$

For the most important cases of application, it is valid to assume $\beta a \ll 1$, whereupon we can use the Bessel function simplification for small arguments to obtain for $R_{13}{}^s$ the formula,

$$R_{13}{}^s = \frac{1}{4\pi d_{s1}\sigma_1}, \quad (32)$$

which has the surprising characteristic of being independent of the radius of the interface. It is obvious that the expression for $R_{32}{}^s$ is similarly given,

$$R_{32}{}^s = \frac{1}{4\pi d_{s2}\sigma_2}. \quad (33)$$

For (32) and (33), σ_1 and σ_2 refer to the conductivities of regions 1 and 2, respectively; likewise, d_{s1} and d_{s2} refer to the skin depths of regions 1 and 2 as evaluated by (28). If the formula for d_s from (28) be substituted into (32) and (33), we obtain an expression for the total interface I^2R loss.

$$R_{13}{}^s + R_{32}{}^s = \frac{1}{4\pi}\left[\sqrt{\frac{\omega\mu_1}{2\sigma_1}} + \sqrt{\frac{\omega\mu_2}{2\sigma_2}}\right]. \quad (34)$$

The contribution due to the flow of surface current in region 2, but for $r > a$, is obtained by substituting

$$I_r{}^s(r) = \frac{I_{z1}}{2\pi r} \quad (35)$$

into (30); and again using R^s from (27) we obtain

$$R_{sk}{}^s = \frac{1}{2\pi d_{s2}\sigma_2}\ln\left(\frac{b}{a}\right). \quad (36)$$

Finally, the total series resistance[3] of a large area varactor diode which can be represented by Fig. 1, is given as

$$R_s = \frac{1}{4\pi}\left\{\sqrt{\frac{\omega\mu_1}{2\sigma_1}}\left(1 + \frac{2w}{a}\right) + \sqrt{\frac{\omega\mu_2}{2\sigma_2}}\left[1 + 2\ln\left(\frac{b}{a}\right)\right]\right\}. \quad (37)$$

Equation (37) reflects the fact that we had previously made the assumption that the media of regions 1 and 2 are relatively good conductors. That is, the inequality

$$\frac{\omega\epsilon}{\sigma} \ll 1 \quad (38)$$

holds in both regions. Alternatively, it is said that the displacement currents are negligible when compared to the conduction currents.

The effect of non-negligible displacement currents will be discussed in a later section.

C. The Point-Contact Diode

Skin effect at a metal-semiconductor contact has already been briefly examined [6]. The intent of that examination was to determine the spatial distribution of current at the contact. A very simple model was considered. It consisted of two semi-infinite right circular cylinders, one of metal, the other of semiconductor having the same diameter as the metal, and connected coaxially with a nonrectifying butt joint. The results are given in reference to cylinders of diameters comparable to the diameter of the point of the practical point-contact diode. It is shown that the redistribution of current flow lines from a decided skin effect in the metal to a negligible effect in the semiconductor takes place mostly in the metal. Thereafter, it is concluded that, "the skin effect is entirely negligible for all point-contact rectifiers at any microwave frequency and the current flow at the contact may be treated with the dc approximation." Not considered was the fact that the current fans out in the semiconductor, and, when skin effects set in, the total spreading resistance increases by the fan-outs becoming extreme to the point of crowding the current lines up to the surface of the semiconductor.

This section will deal with the problem of the point-contact diode, and we will derive a fairly rigorous expression for the spreading resistance which will include both frequency dependent (skin effect) terms and terms involving the semiconductor geometry. It will be further shown that the junction will definitely behave just as at dc, but that there is a significant correction to be made to R_s because of skin effect.

1) *The Natural Coordinate System:* The previously noted analysis and others which have similar configuration have contained drastic simplifications due to the complexity of exact analysis in cylindrical coordinates, which system, because of the physical configuration, one would consider the most applicable. But if one considers the dc case, it may be shown that the oblate spheroidal coordinate system is the natural system as the current flow lines coincide with the coordinate system. Allow Fig. 3 to define the coordinate system [9].

The rectangular (x, y, z) coordinates are related to the (ξ, η, ϕ) oblate spheroidal coordinates by the formulas

$$x = a[(1 - \eta^2)(\xi^2 + 1)]^{1/2}\cos\phi \quad (39)$$

$$y = a[(1 - \eta^2)(\xi^2 + 1)]^{1/2}\sin\phi \quad (40)$$

$$z = a\eta\xi \quad (41)$$

where

$$0 \le \eta \le 1, \qquad -\infty < \xi \le 0, \qquad 0 \le \phi \le 2\pi.$$

[3] An expression for R_s for the broad area varactor was first presented by Hines [11]. Details of his derivation are not available but it appears that only the interface contribution was considered. Hines gives

$$R_s = \frac{1}{8}\sqrt{\frac{f\mu}{\pi}}\left(\frac{1}{\sqrt{\sigma_1}} + \frac{1}{\sqrt{\sigma_2}}\right).$$

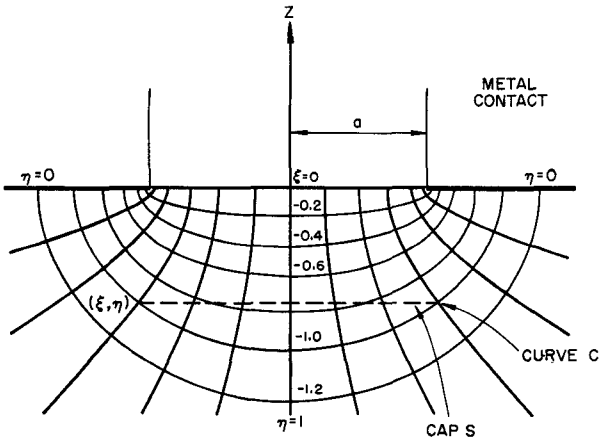

Fig. 3. Oblate spheroidal coordinate system.

The metrical coefficients are given as

$$h_1 = a\left(\frac{\xi^2 + \eta^2}{\xi^2 + 1}\right)^{1/2}, \tag{42}$$

$$h_2 = a\left(\frac{\xi^2 + \eta^2}{1 - \eta}\right)^{1/2} \tag{43}$$

and

$$r = a[(1 - \eta^2)(\xi^2 + 1)]^{1/2}. \tag{44}$$

Laplace's equation, $\nabla^2 V = 0$, is given in oblate spheroidal coordinates as

$$\left[\frac{\partial}{\partial \eta}(1 - \eta^2)\frac{\partial}{\partial \eta} + \frac{\partial}{\partial \xi}(\xi^2 + 1)\frac{\partial}{\partial \xi}\right] V = 0, \tag{45}$$

where the ϕ dependence has already been set equal to zero. The contact surface, taken to be the disk of radius a at $\xi = 0$, is at constant potential V_0. Since the contact disk is equipotential, then Laplace's equation shows that $(\partial V/\partial \eta) = 0$ must hold through the entire region and the potential V, must therefore be independent of η. Equation (45) then reduces to

$$\left[\frac{\partial}{\partial \xi}(\xi^2 + 1)\frac{\partial}{\partial \xi}\right] V = 0, \tag{46}$$

which has the solution of the form

$$V(\xi) = C_1 \tan^{-1} \xi + C_2, \tag{47}$$

where C_1 and C_2 are constants of integration. If we take $V = V_0$ at $\xi = 0$ and $V = 0$ at $\xi = -\infty$, it can be shown that

$$V(\xi) = V_0\left[1 + \frac{2}{\pi}\tan^{-1} \xi\right]. \tag{48}$$

The current density is $J = -\sigma \nabla V$ which is

$$J = -\frac{\sigma}{h_1}\frac{\partial V(\xi)}{\partial \xi} \tag{49}$$

and by using (42) and (48), J becomes at the disk electrode ($\xi = 0$)

$$J = \frac{-2V_0\sigma}{\pi a \eta}. \tag{50}$$

Integrating this current density over the surface of the disk one obtains the total current I_T which allows the calculation of the spreading resistance $R = V_0/I_T$.

$$I_T = 4V_0\sigma a. \tag{51}$$

Thus,

$$R_s = \frac{1}{4\sigma a}, \tag{52}$$

is the resistance between the source electrode and the sink at infinity. This is the expression for spreading resistance most often encountered in the literature.

2) *Field Equations in the Oblate Spheroidal Systems:* To extend these considerations to the determination of the skin effect, we return to the use of the scalar function Q. If the metrical coefficients as given in (42)–(44) are substituted into the differential equation (10), there is obtained the differential equation for Q which must be satisfied when Q is described in the oblate spheroidal coordinate system,

$$(\xi^2 + 1)\frac{\partial^2 Q}{\partial \xi^2} + (1 - \eta^2)\frac{\partial^2 Q}{\partial \eta^2} - a^2\gamma^2(\xi^2 + \eta^2)Q = 0. \tag{53}$$

Use of

$$Q(\xi, \eta) = Q(\eta)\, Q(\xi) \tag{54}$$

leads to a solution of (53) of the following as

$$Q(\xi, \eta) = A_1 e^{a\gamma\eta\xi} + e^{a\gamma\xi}[A_2 e^{ja\gamma\eta} + A_3 e^{-ja\gamma\eta}] \tag{55}$$

where the coefficients A_1, A_2, and A_3 are arbitrary constants.

It is recognized that solutions of (53) via the procedure of separation of variables are infinite in number and may be obtained in the form of Lamé products [9] but it can be shown that the form given in (55) is sufficient to satisfy the boundary conditions on Q and that $Q(\xi, \eta)$ can take the following form

$$Q(\xi, \eta) = \frac{I_T}{2\pi}\left[e^{a\gamma\eta\xi} - e^{a\gamma\xi}\frac{\sin(a\gamma\eta)}{\sin(a\gamma)}\right]. \tag{56}$$

From (8) and (9) the electric intensities are found to be

$$E_\xi(\xi, \eta) = \frac{j\omega\mu}{a\gamma}\frac{(I_T/2\pi)}{\sqrt{(\xi^2 + 1)(\xi^2 + \eta^2)}} \cdot \left[\xi e^{a\gamma\eta\xi} - e^{a\gamma\xi}\frac{\cos(a\gamma\eta)}{\sin(a\gamma)}\right] \tag{57}$$

and

$$E_\eta(\xi, \eta) = \frac{-j\omega\mu}{a\gamma}\frac{(I_T/2\pi)}{\sqrt{(1 - \eta^2)(\xi^2 + \eta^2)}} \cdot \left[\eta e^{a\gamma\eta\xi} - e^{a\gamma\xi}\frac{\sin(a\gamma\eta)}{\sin(a\gamma)}\right]. \tag{58}$$

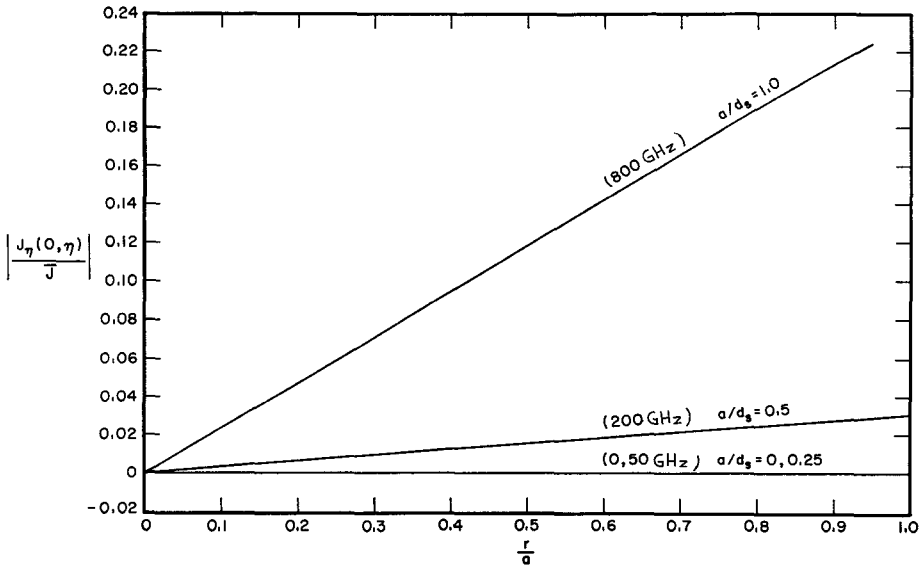

Fig. 4. Normalized radial current density J_η versus fractional radius.

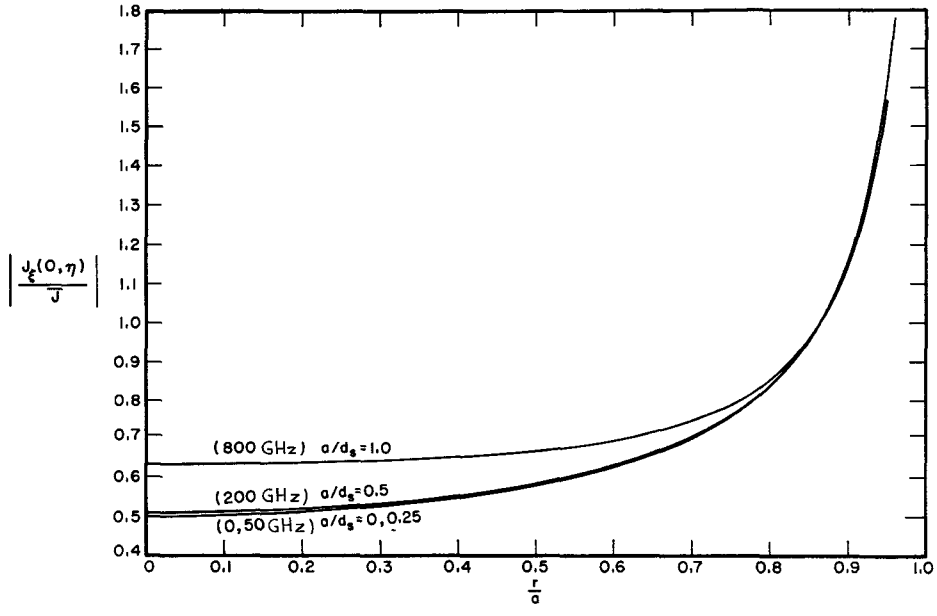

Fig. 5. Normalized axial current density J_ξ versus fractional radius.

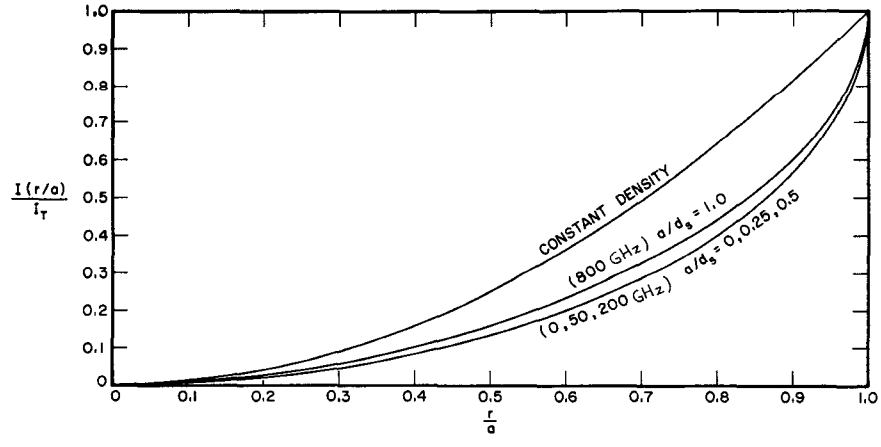

Fig. 6. Normalized total current distribution $I(r/a)$ versus fractional radius.

3) *Current Distribution:* The current densities are given by

$$J_\xi(\xi, \eta) = \frac{a\gamma I_T}{2\pi a^2} \frac{1}{\sqrt{(\xi^2+1)(\xi^2+\eta^2)}} \cdot \left[\xi e^{a\gamma\eta\xi} - e^{a\gamma\xi}\frac{\cos(a\gamma\eta)}{\sin(a\gamma)}\right] \quad (59)$$

and

$$J_\eta(\xi, \eta) = \frac{-a\gamma I_T}{2\pi a^2} \frac{1}{\sqrt{(1-\eta^2)(\xi^2+\eta^2)}} \cdot \left[\eta e^{a\gamma\eta\xi} - e^{a\gamma\xi}\frac{\sin(a\gamma\eta)}{\sin(a\gamma)}\right]. \quad (60)$$

Equations (59) and (60) were evaluated at the contact surface $\xi=0$. An average current density, $\bar{J}=I_T/\pi a^2$, is defined after which the ratios $J_\xi/\bar{J}$ and $J_\eta/\bar{J}$ were calculated for various points across the contact and the results plotted versus (r/a), the fractional radius. Again the assumption is made that the material is a relatively good conductor. Then as

$$a\gamma = (1+j)\frac{a}{d_s}, \quad (61)$$

where d_s is from (28), the normalized current densities can be plotted as a function of the ratio a/d_s, which is the ratio of contact radius to bulk material skin depth. Figures 4 and 5 show $J_\eta/\bar{J}$ and $J_\xi/\bar{J}$, respectively, for three values of a/d_s. But note in each case (as was calculated) there was no significant difference between the case for $(a/d_s)=0.25$ and $(a/d_s)=0$. The latter case obviously is the dc case, and the curve of $J_\xi/\bar{J}$ is just that which would be obtained by plotting (50) vs. r/a. But the case (which does not measurably differ from the dc case) $(a/d_s)=0.25$ corresponds to an extreme case determined by the conditions:

a) frequency of 50 GHz.

b) a contact radius $a=0.05$ mil. This is representative of typical microwave and millimeter wave point-contact diodes [8], [12].

c) bulk semiconductor resistivity $\rho=0.0005$ ohm-cm.

This figure represents the resistivity that would be encountered in millimeter wave-tunnel diodes and is from one to two orders of magnitude lower than that encountered in the more conventional point-contact diodes.

Inspection of the curve for J_η shows that essentially $J_\eta=0$ for $(a/d_s)\leq 0.25$ and becomes measurable only when $(a/d_s) \doteq 0.5$. But for the same conditions as in b) and c) above, this (a/d_s) ratio corresponds to a frequency range of 200 GHz. Further, as the I^2R contribution due to J_η will be less than 0.1 percent of that due to J_ξ, it would appear that even to this extreme value of (a/d_s) the current density expressions are good, and the contact still represents an equipotential.

The curves for $(a/d_s)=1.0$ show much more deviation for J_η, and its I^2R contribution now becomes about 5 percent. But this figure, $(a/d_s)=1.0$, corresponds to a frequency of 800 GHz which is quite beyond the range of anticipated application of these results.

In addition to the curves for J_η and J_ξ, the curves showing the actual current distribution are shown in Fig. 6. In this figure $I(r/a)$ is the total current entering the electrode in a circle of radius r. This is then normalized to the total current I_T. Notice that the curves for $(a/d_s)=0$, 0.25, and 0.5 essentially coincide (within the plotting ability), and that no appreciable redistribution of the current occurs until (a/d_s) becomes greater than 0.5. The data for $(a/d_s)=1$, which corresponds to a frequency of 800 GHz for this case, begin to show deviations, but are still far below the curve shown for the case of constant current density.

With this development and this discussion it is believed that the statement, "at the junction, the current flow may be treated with the dc approximation," has been sufficiently and rigorously proven. In addition, meaning is given to the statement, because now the equations exist which allow the evaluation of the associated spreading resistance, and make it unnecessary to assume that, because the junction can be treated with the dc approximation, the rest of the problem can be also.

4) *Spreading Resistance:* To obtain the spreading resistance with the skin effect contribution the following assumption will be made; that the wafer of semiconductor material, rather than being considered the infinite half space, have a definite radius b, and that the thickness of the wafer be appreciably greater than the skin depth in the wafer. Except for diodes constructed on epitaxial materials this is a good assumption. Allow Fig. 7 to show the situation. Region 1 represents the metal point contact. Region 2 is the semiconductor buried in the metal, high conductance return path 3. If the metal regions are of sufficiently high conductance relative to the semiconductor, then the principal potential drop will be across the semiconductor. If the expressions for the electric intensities (57) and (58) are examined, it can be seen that, for $\xi \gg 1$ and for $z=0$ $(a\eta\xi=0)$, E_η vanishes and that near the semiconductor surface the current flow I_r becomes strictly radial, as illustrated in Fig. 7, hence the validity and necessity of applying the realistic condition at $r=b$. The potential drop across the semiconductor from $r=a$ to $r=b$ can be taken as

$$V = -\int_b^a E_\xi(\xi, 0)dr, \quad (62)$$

where the integration proceeds along any one radial line because of the cylindrical symmetry of the situation.

Now after some manipulation of (57) in (62) the expression for the impedance Z can be shown to be

$$Z = \frac{(1+j)}{2\pi\sigma d_s}\ln\left(\frac{b}{a}\right) + \frac{1}{2\pi\sigma a}\tan^{-1}\left(\frac{b}{a}\right). \quad (63)$$

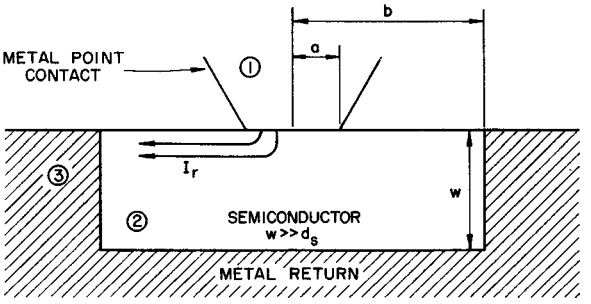

Fig. 7. Point contact with skin effect.

Agreement is obtained with the dc case with infinite half space of semiconductor, by noting that as $(b/a)\rightarrow\infty$ and frequency $\omega\rightarrow 0$ we have

$$\tan^{-1}\left(\frac{b}{a}\right)\rightarrow\frac{\pi}{2} \quad \text{as} \quad \left(\frac{b}{a}\right)\rightarrow\infty \tag{64}$$

and

$$d_s\rightarrow\infty \quad \text{as} \quad \omega\rightarrow 0, \tag{65}$$

yielding, in the limit

$$\lim_{\substack{\omega\rightarrow 0\\ b/a\rightarrow\infty}} Z=\frac{1}{4\sigma a} \tag{66}$$

which agrees with (52).

The real part of Z can now be taken to be the total spreading resistance R_s of the device shown in Fig. 7. Thus,

$$R_s=\frac{1}{2\pi\sigma}\left[\frac{1}{d_s}\ln\left(\frac{b}{a}\right)+\frac{1}{a}\tan^{-1}\left(\frac{b}{a}\right)\right], \tag{67}$$

and

$$R_s=\frac{1}{2\pi}\left[\sqrt{\frac{\omega\mu}{2\sigma}}\ln\left(\frac{b}{a}\right)+\frac{1}{\sigma a}\tan^{-1}\left(\frac{b}{a}\right)\right]. \tag{68}$$

III. Conduction Currents Versus Displacement Currents

In all the calculations and discussion in the paper involving the skin depth d_s, the assumption has been made that the region of interest was composed of a "reasonably" good conductor, and thus the ratio β of the magnitudes of the displacement to conduction currents was taken to be zero. If such is not the case the attenuation term $\mathrm{Re}\{\gamma z\}$ must be re-examined. If we call δ the true skin depth then

$$\delta=\frac{1}{\mathrm{Re}\{\gamma\}}. \tag{69}$$

As γ is the intrinsic propagation constant then γ^2 is given by

$$\gamma^2=j\omega\mu(\sigma+j\omega\epsilon) \tag{70}$$

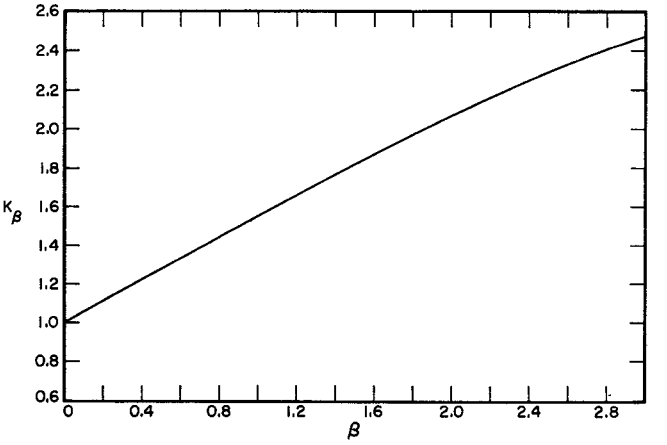

Fig. 8. Scale factor K_β due to non-negligible displacement current.

and for $\mathrm{Re}\{\gamma\}$ it may be shown that

$$\mathrm{Re}\{\gamma\}=\frac{\sqrt{2}}{d_s}(1+\beta^2)^{1/4}\cos\left[\frac{1}{2}\left(\frac{\pi}{2}+\tan^{-1}\beta\right)\right] \tag{71}$$

where β is defined to be

$$\beta=\frac{\omega\epsilon}{\sigma}, \tag{72}$$

where $\epsilon=\epsilon_0\epsilon_r$, in which ϵ_0 and ϵ_r are the permittivity of free space and the relative permittivity (dielectric constant), respectively. σ, as was defined previously, is the conductivity of the material, d_s is the skin depth (28) as calculated for $\beta=0$, and is shown in Fig. 2.

Now the true skin depth δ is given by

$$\delta=K_\beta d_s, \tag{73}$$

where the scale factor K_β is taken from (71) and is

$$K_\beta=\left\{\sqrt{2}(1+\beta^2)^{1/4}\cdot\cos\left[\frac{1}{2}\left(\frac{\pi}{2}+\tan^{-1}\beta\right)\right]\right\}^{-1}. \tag{74}$$

K_β is plotted versus β and presented in Fig. 8. In all the cases where the term d_s was used, if it be necessary, the corrected term δ may be obtained by evaluating K_β (reading from Fig. 8) and scaling d_s accordingly. In all cases, the skin effect term of the spreading resistance is inversely proportional to K_β, and thus the correction applies directly to the resistance term.

To demonstrate the general range of β, we compute for a semiconductor of $\epsilon_r=16$ and conductivity $\sigma=1$ mho/cm and a frequency of 100 GHz, and obtain $\beta\doteq 1.0$. For these conditions the true skin depth δ will be about 60 percent greater than that value d_s, normally used. But it should also be pointed out that a very high frequency was taken and that the material resistivity was at least one order of magnitude too high for the usual millimeter wave point-contact diode and as much as three orders of magnitude higher than the resistivity needed for the fabrication of high-frequency point-

contact tunnel diodes. By these arguments it is seen that for most high-frequency diode calculations the correction need not be applied. Similar arguments apply when the spreading resistance with skin effect is being considered in a transistor. While the resistivity of the transistor material may be one to two orders of magnitude higher than in a microwave diode, the frequency of operation is usually two to three orders of magnitude less than the 100 GHz figure used here. Again the correction term should prove negligible.

IV. Conclusions

Equations for the spreading resistance of the broad area variable-capacitance diode and the point-contact variable-resistance diode have been derived in terms of frequency, material characteristics (μ, ϵ, σ), and physical parameters (b/a) and (w/a). The results are presented in (37) and (68).

The field equations for the point-contact diode configuration have been derived in terms of the oblate spheroidal coordinates. It has been shown that this is the natural coordinate system for such an analysis and that the spreading resistance is quite readily derived in this system.

A discussion is presented which shows that the effects of displacement current in the semiconductor are, in most instances, negligible in comparison to the conduction currents.

References

[1] R. W. P. King, *Electromagnetic Engineering*. New York: McGraw-Hill, 1945.

[2] L. E. Dickens, "Spreading resistance as a function of geometry" (to be published). Both papers based on Tech. Rept. NAS-1, prepared for NASA/GSFC under Contract NAS 5-3546, and Tech. Doc. Rept. AL-TDR-64-240, prepared for AFAL/RTD under Contract AF 33(657)-11029.

[3] R. Holm, *Electric Contacts*. Stockholm: Hugo Gebers Forlag, 1946.

[4] J. A. Stratton, *Electromagnetic Theory*. New York: McGraw-Hill, 1941.

[5] E. Jahnke and F. Emde, *Tables of Functions*. New York: Dover, 1945.

[6] L. A. Blackwell and K. L. Kotzebue, *Semiconductor-Diode Parametric Amplifiers*. Englewood Cliffs, N. J.: Prentice-Hall, 1961.

[7] K. K. N. Chang, *Parametric and Tunnel Diodes*. Englewood Cliffs, N. J. Prentice-Hall, 1964.

[8] H. C. Torrey and C. A. Whitmer, *Crystal Rectifiers*. New York: McGraw-Hill, 1948.

[9] C. Flammer, *Spheroidal Wave Functions*, A Stanford Research Inst. Monograph. Stanford, Calif.: Stanford University Press, 1957.

[10] G. A. Korn and T. M. Korn, *Mathematical Handbook for Scientists and Engineers*. New York: McGraw-Hill, 1961.

[11] M. E. Hines, "High frequency limitations of solid-state devices and circuits," a Discourse presented to the International Solid-State Circuits Conference, Univ. of Pa., Philadelphia, 1963.

[12] W. M. Sharpless, "Gallium-arsenide point-contact diodes," *IRE Trans. on Microwave Theory and Techniques*, vol. MTT-9, pp. 6–10, January 1961.

An Exact Calculation for a *T*-Junction of Rectangular Waveguides Having Arbitrary Cross Sections

EUGENE D. SHARP, MEMBER, IEEE

Abstract—**An exact method is developed for the calculation of the electrical performance of the rectangular waveguide *T*-junction. This method is used to find the equivalent circuit of a rectangular waveguide *T*-junction in which both cross-sectional dimensions of the side waveguide are different from the cross-sectional dimensions of the through waveguide. The theoretical calculations for a particular *T*-junction of this type are verified by experimental measurements. In this method the electrical performance is analyzed by using equivalent-circuit concepts applied to waveguide modes to calculate an admittance matrix relating propagating and cutoff waveguide modes to each other. Then the cutoff modes are terminated in their characteristic impedance, and an equivalent admittance matrix of the junction is found relating only the propagating modes in each waveguide to each other. The analysis is valid when any number of modes can propagate in the waveguides forming the junction. The inversion of an infinite matrix is required; however, any desired accuracy can be obtained by considering a matrix of finite but sufficient size or equivalently by considering a sufficient number of cutoff modes.**

Manuscript received March 25, 1966; revised September 30, 1966. The work reported in this paper was performed while the author was at Stanford Research Institute and was reported in a Technical Note for Rome Air Development Center, Rome, N. Y.

The author is with TRG-West, Incorporated, Menlo Park, Calif., a subsidiary of Control Data Corporation.

I. Introduction

IN THE PAST few years, interest has been shown in waveguide filters that employ waveguides operating below cutoff. Experimental data have been published giving the performance of a reactive filter consisting of an *E*-plane *T*-junction in which the side waveguide of the junction is of a smaller cross section than the through waveguide [1]. The side arm is short circuited a distance from the junction. This structure acts as a narrowband reject filter with the rejection band centered just above the side waveguide cutoff frequency.

The same type junction has been used in waveguide low-pass dissipative filters. Instead of being short circuited, the